

© 2013 IEEE. Personal use of this material is permitted. Permission from IEEE must be obtained for all other uses, in any current or future media, including reprinting/republishing this material for advertising or promotional purposes, creating new collective works, for resale or redistribution to servers or lists, or reuse of any copyrighted component of this work in other works.

Digital Object Identifier (DOI): [10.1109/APEC.2013.6520231](https://doi.org/10.1109/APEC.2013.6520231)

IEEE

Power Controllability of Three-phase Converter with Unbalanced AC Source

Ke Ma
Frede Blaabjerg
Marco Liserre

Suggested Citation

K. Ma, F. Blaabjerg, M. Liserre, "Power Controllability of Three-phase Converter with Unbalance AC Source," Proc. of APEC' 2013

Power Controllability of Three-phase Converter with Unbalanced AC Source

Ke Ma, Marco Liserre, Frede Blaabjerg

Department of Energy Technology, Aalborg University
 Pontoppidanstraede 101, DK-9220 Aalborg East, Denmark
kema@et.aau.dk, mli@et.aau.dk, fbl@et.aau.dk

Abstract – Three-phase DC-AC power converters suffer from power oscillation and overcurrent problems in case of unbalanced AC source voltage that can be caused by grid/generator faults. Existing solutions to handle these problems are properly selecting and controlling the positive and negative sequence currents. In this work a new series of control strategies which utilize the zero-sequence components are proposed to enhance the power control ability under this adverse condition. It is concluded that by introducing proper zero sequence current controls and corresponding circuit configurations, the power converter can enable more flexible control targets, achieving better performances in the delivered power and load current when suffering from unbalanced AC source.

Keywords: DC-AC converter, Unbalanced AC source, Control strategy, Fault tolerance

I. INTRODUCTION

In many important applications for power electronics such as power generation, motor drives, power quality, etc., the three-phase DC-AC converters are important part as the backbone interface between DC and AC electrical systems [1], [2]. As shown in Fig. 1, a typical DC-AC voltage source converter is used to convert the energy between the DC bus and the three-phase AC sources, which could be the power grid, generation units or the electric machines depending on the applications [3]-[5].

Since the power electronics are getting so widely used

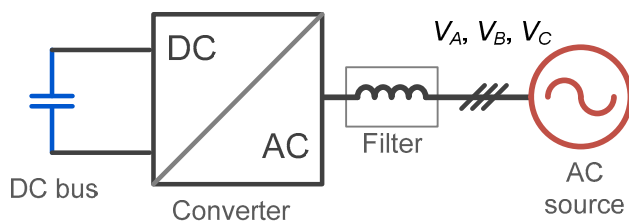


Fig. 1. A typical DC-AC converter application.

and becoming essential in the energy conversion technology, the failures or shutting down of these backbone DC-AC converters may result in serious problems and cost. It is becoming a need in many applications that the power converters should be reliable to withstand some faults or disturbances in order to ensure certain availability of the energy supply [6]-[13].

When the voltages become distorted and unbalanced under faults or disturbances, the unbalanced AC voltages have been proven to be a great challenge for the control of DC-AC converters in order to keep them normally operating and connected to the AC sources [2], [14], [15]. Special control methods which can regulate both the positive and negative sequence currents have been introduced to handle these problems [2], [16]-[21]. However, the resulting performances by these control methods are not satisfactory: either distorted load currents or power oscillations will be introduced, and thereby not only the grid/generator but also the power converter will be further stressed.

This paper targets to improve the power control limits of typical three-phase DC-AC converter system under unbalanced AC source (e.g. grid or generator with voltage dips). A new series of control strategies which utilizes the zero-sequence components are then proposed to enhance the power control ability under this adverse condition.

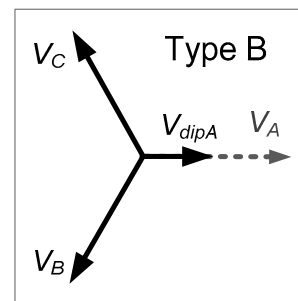


Fig. 2. Phasor diagram definitions for the voltage dips in the AC source of Fig. 1. V_A, V_B, V_C means the voltage of three phases in the AC source.

II. LIMITS OF TYPICAL THREE-WIRE CONVERTER SYSTEM

In order to analyze the control ability and performance of power converter under adverse AC source condition, a distorted source voltage is first defined as a case study in this paper. As shown in Fig. 2, the phasor diagram of the three phase distorted voltage are indicated, it is assumed that the type B fault happens in the AC source with significant voltage dip on phase A. Also there are many other types of voltage faults which are defined as type A-F in [22].

According to [2], [19], any distorted three-phase voltage can be expressed by the sum of components in positive sequence, negative sequence and zero sequence. For simplicity of analysis only the components with fundamental frequency are considered in this paper, however it is also possible to extend the analysis to higher order harmonics. The distorted three-phase AC source voltage in Fig. 2 can be represented by:

$$\begin{aligned} \mathbf{V}_s &= \mathbf{V}^+ + \mathbf{V}^- + \mathbf{V}^0 \\ &= \begin{bmatrix} v_a \\ v_b \\ v_c \end{bmatrix} = V^+ \begin{bmatrix} \sin(\omega t + \varphi^+) \\ \sin(\omega t - 120^\circ + \varphi^+) \\ \sin(\omega t + 120^\circ + \varphi^+) \end{bmatrix} \\ &\quad + V^- \begin{bmatrix} \sin(\omega t + \varphi^-) \\ \sin(\omega t + 120^\circ + \varphi^-) \\ \sin(\omega t - 120^\circ + \varphi^-) \end{bmatrix} + V^0 \begin{bmatrix} \sin(\omega t + \varphi^0) \\ \sin(\omega t + \varphi^0) \\ \sin(\omega t + \varphi^0) \end{bmatrix} \end{aligned} \quad (1)$$

where V^+ , V^- and V^0 are the voltage amplitude in positive, negative and zero sequence respectively. And φ^+ , φ^- and φ^0 represent the initial phase angles in positive sequence, negative sequence and zero sequence respectively. The predefined single phase voltage dip as indicated in Fig. 2 should contain voltage components in all the three sequences [2], [11].

A typical used three-phase three-wire two-level voltage source DC-AC converter is chosen and basically designed, as shown in Fig. 3 and Table I, where the converter configuration and the parameters are indicated respectively. It is noted that the three-phase AC source is represented here by three windings with a common neutral point, which can be the windings of electric machine or transformer.

Because there are only three-wires and a common neutral point in the windings of AC source, the currents flowing in the three phases don't contain zero sequence components. As a result the three-phase load current controlled by the converter can be written as:

$$\mathbf{I}_c = \mathbf{I}^+ + \mathbf{I}^- \quad (2)$$

With the voltage of AC source in (1) and current controlled by converter in (2), the instantaneous real power p and imaginary power q in $\alpha\beta$ coordinate, as well as the real power p_0 in the zero coordinate can be calculated as:

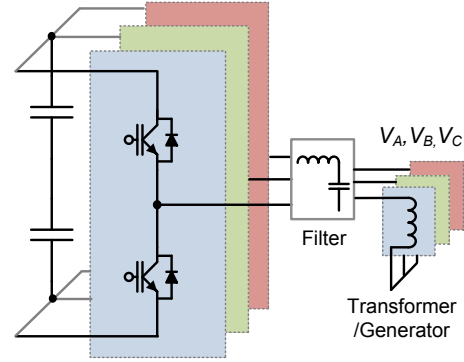


Fig. 3. Typical three-phase three-wire 2L VSC.

Table I. Converter parameters for case study.

Rated output active power P_o	10 MW
DC bus voltage V_{dc}	5.6 kV DC
*Rated primary side voltage V_p	3.3 kV rms
Rated line-to-line grid voltage V_g	20 kV rms
Rated load current I_{load}	1.75 kA rms
Carrier frequency f_c	750 Hz
Filter inductance L_f	1.1 mH (0.25 p.u.)

* Line-to-line voltage in the primary windings of transformer.

$$\begin{aligned} \begin{bmatrix} p \\ q \\ p_0 \end{bmatrix} &= \begin{bmatrix} v_\alpha \cdot i_\alpha + v_\beta \cdot i_\beta \\ v_\alpha \cdot i_\beta - v_\beta \cdot i_\alpha \\ v_0 \cdot 0 \end{bmatrix} \\ &= \begin{bmatrix} \bar{P} + P_{c2} \cdot \cos(2\omega t) + P_{s2} \cdot \sin(2\omega t) \\ \bar{Q} + Q_{c2} \cdot \cos(2\omega t) + Q_{s2} \cdot \sin(2\omega t) \\ 0 \end{bmatrix} \end{aligned} \quad (3)$$

Then the instantaneous three phase real power $p_{3\phi}$ and imaginary power $q_{3\phi}$ of the AC source/converter can be written as:

$$\begin{bmatrix} p_{3\phi} \\ q_{3\phi} \end{bmatrix} = \begin{bmatrix} \bar{P} \\ \bar{Q} \end{bmatrix} + \begin{bmatrix} P_{c2} \\ Q_{c2} \end{bmatrix} \cos(2\omega t) + \begin{bmatrix} P_{s2} \\ Q_{s2} \end{bmatrix} \sin(2\omega t) \quad (4)$$

where \bar{P} and \bar{Q} is the average part of the real and imaginary power, P_{c2} , P_{s2} and Q_{c2} , Q_{s2} are the oscillation parts, which can be calculated as:

$$\begin{aligned}\overline{P} &= \frac{3}{2}(v_d^+ \cdot i_d^+ + v_d^- \cdot i_d^-) \\ P_{c2} &= \frac{3}{2}(v_d^- \cdot i_d^+ + v_d^+ \cdot i_d^-)\end{aligned}\quad (5)$$

$$\begin{aligned}P_{s2} &= \frac{3}{2}(-v_d^- \cdot i_q^+ + v_d^+ \cdot i_q^-) \\ \overline{Q} &= \frac{3}{2}(-v_d^+ \cdot i_q^+ - v_d^- \cdot i_q^-) \\ Q_{c2} &= \frac{3}{2}(-v_d^- \cdot i_q^+ - v_d^+ \cdot i_q^-)\end{aligned}\quad (6)$$

$$Q_{s2} = \frac{3}{2}(-v_d^- \cdot i_d^+ + v_d^+ \cdot i_d^-)$$

where

$$\begin{aligned}v_d^+ &= V^+ \cos(\varphi^+) = V^+ & i_d^+ &= I^+ \cos(\delta^+) \\ v_q^+ &= V^+ \sin(\varphi^+) = 0 & i_q^+ &= I^+ \sin(\delta^+) \\ v_d^- &= V^- \cos(\varphi^-) = V^- & i_d^- &= I^- \cos(\delta^-) \\ v_q^- &= -V^- \sin(\varphi^-) = 0 & i_q^- &= -I^- \sin(\delta^-)\end{aligned}\quad (7)$$

It can be seen from (5) and (6) that if the AC source voltage is decided, then the converter has four controllable freedoms (i_d^+ , i_q^+ , i_d^- and i_q^-) to regulate the current flowing in the AC source. That also means: four control targets/functions can be established. Normally the three-phase average active and reactive powers delivered by the converter are two basic requirements for a given application, then two basic control functions have to first be settled as:

$$\begin{aligned}\overline{P}_{3\phi} &= \overline{P} = P_{ref} \\ \overline{Q}_{3\phi} &= \overline{Q} = Q_{ref}\end{aligned}\quad (8)$$

Different applications may have different requirements for the average power. For the power generation application, the active power reference P_{ref} is set as negative, meanwhile large amount of reactive power Q_{ref} may be needed in order to help the grid recover from voltage dips [12], [13]. As for the electric machine application, the P_{ref} is set as negative for generator mode and positive for motor mode, there may be no or a few reactive power Q_{ref} requirements for magnetizing. While in most power quality applications e.g. STACOM, P_{ref} is normally set to be very small to provide low converter loss, and a large amount of Q_{ref} is normally required.

Consequently, for the three-phase three-wire converter system there are only two more current control freedoms left to achieve another two control targets besides (8). These two adding control targets may be utilized to further improve the performances of the converter under unbalanced AC source. In the following the potential control performances achieved by three-wire converter structure are illustrated.

A. Elimination of negative sequence current

In most of the grid integration applications, there are strict grid codes to regulate the behavior of the grid connected converters. The negative sequence current which always results in unbalanced load current may be unacceptable from the point view of Transmission System Operator (TSO) [13]. Therefore, extra two control targets which aim to eliminate the negative sequence current can be added as:

$$\begin{aligned}i_d^- &= 0 \\ i_q^- &= 0\end{aligned}\quad (9)$$

Translating the control targets in (8) and (9), all the controllable current components can be calculated as:

$$\begin{aligned}i_d^+ &= \frac{2}{3} \cdot \frac{P_{ref}}{v_d^+ - v_d^-} & i_d^- &= 0 \\ i_q^+ &= -\frac{2}{3} \cdot \frac{Q_{ref}}{v_d^+} & i_q^- &= 0\end{aligned}\quad (10)$$

When applying the current references in (10), the source voltage, load current, sequence current amplitude, and the instantaneous power delivered by the converter are shown in Fig. 4. The simulation is based on the parameters predefined in Fig. 1 and Table I. The AC source voltage is set with V_A dipping to zero. The average active power reference P_{ref} for the converter is set as 1 p.u. and reactive power reference Q_{ref} is set as 0.

It can be seen from Fig. 4 that with the extra control targets in (9), there is no zero sequence nor negative sequence components in the load current, i.e. the currents among the three phases of converter are symmetrical under the given extreme unbalanced AC source condition.

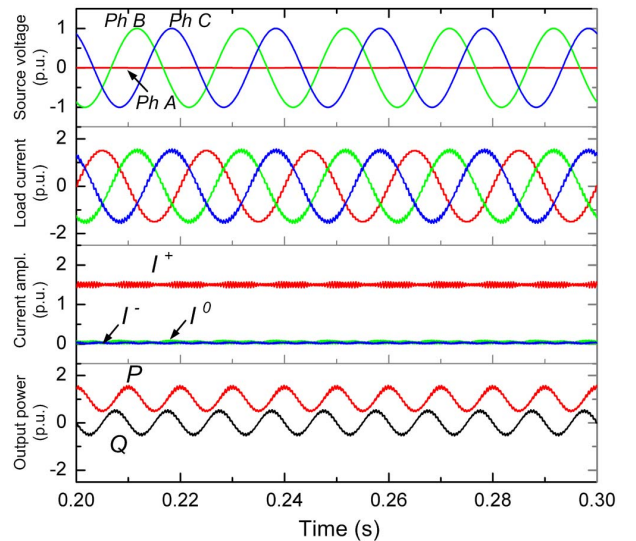
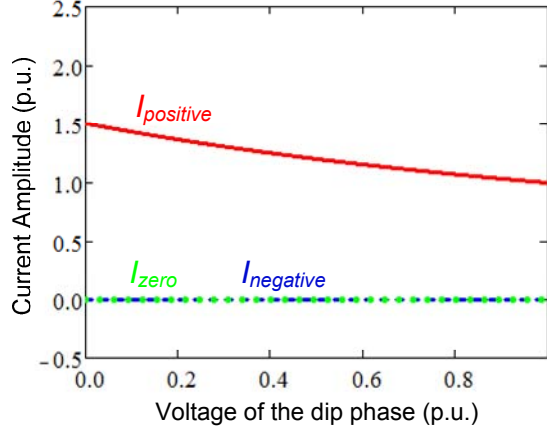
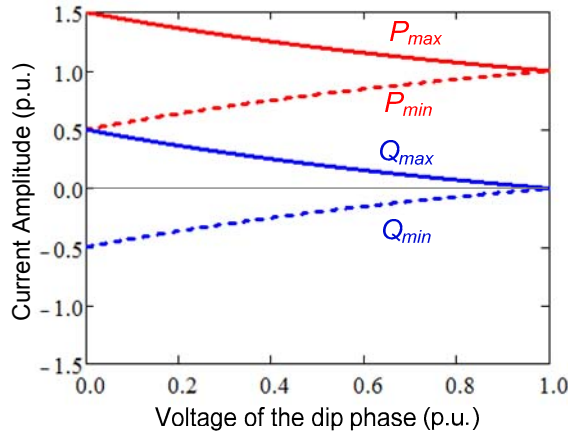


Fig. 4. Simulation of the converter with no negative sequence current control (three phase three-wire converter, $P_{ref}=1$ p.u., $Q_{ref}=0$ p.u., $I_d^-=0$ p.u., $I_q^-=0$ p.u., $V_A=0$ p.u.)



(a) Sequence current amplitude vs. V_A .



(b) P and Q oscillation range vs. V_A .

Fig. 5. Profile of converter control with no negative sequence current (three phase three-wire converter, $P_{ref}=1$ p.u., $Q_{ref}=0$ p.u., $I_d=0$ p.u., $I_q=0$ p.u.)

The current amplitude in different sequences and the delivered active/reactive power with relation to the voltage amplitude of the dipping phase V_A are shown in Fig. 5 (a), and Fig. 5 (b), respectively. It is noted that only positive sequence current are generated by the converter, and there is up to ± 0.5 p.u. oscillations both in the active and reactive power when V_A dips to zero. The significant fluctuation of active power would result in the voltage fluctuation of the DC bus [16]-[19], compromising not only the THD but also the reliability performances of the converter according to [23].

B. Elimination of active power oscillation

In order to overcome the disadvantage of the active power 1.3oscillation under unbalanced AC source, another two extra control targets which aim to cancel the oscillation items in the instantaneous active power can be used to replace (9) as:

$$\begin{aligned} P_{3\phi c2} &= P_{c2} = 0 \\ P_{3\phi s2} &= P_{s2} = 0 \end{aligned} \quad (11)$$

Translating the control targets in (8) and (11), all the controllable current components of the converter can be calculated as:

$$\begin{aligned} i_d^+ &= \frac{2}{3} \cdot \frac{P_{ref} \cdot v_d^+}{M} & i_d^- &= -\frac{2}{3} \cdot \frac{P_{ref} \cdot v_d^-}{M} \\ i_q^+ &= 0 & i_q^- &= 0 \end{aligned} \quad (12)$$

Where

$$M = [(v_d^+)^2 + (v_q^+)^2] - [(v_d^-)^2 + (v_q^-)^2] \quad (13)$$

When applying the current references in (12) and (13), the corresponding source voltage, load current, sequence current, and the instantaneous power delivered by the converter are shown in Fig. 6. It can be seen that the active power oscillation at twice of the fundamental frequency can be eliminated.

However, the disadvantage of this control strategy is also significant: the converter has to deliver up to 3 p. u. load current in the faulty phase which is much larger than the other two normal phases. Even larger fluctuation of reactive power will be presented compared to the control strategy in Fig. 4.

The current amplitude in the different sequences, as well as the delivered active/reactive power with relation to the voltage amplitude on dipping phase is shown in Fig. 7 (a) and Fig. 7 (b) respectively. It is noted that the converter has to deliver both positive and negative sequence current to achieve this control strategy, and up to ± 1.3 p.u. oscillation in the reactive power is generated when V_A dips to zero.

Another three possible control strategies which can eliminate the oscillation of reactive power as shown in (14), or reduce the oscillations of both active and reactive power as shown in (15) and (16), are also possible for the three-phase three-wire converter under unbalanced AC source:

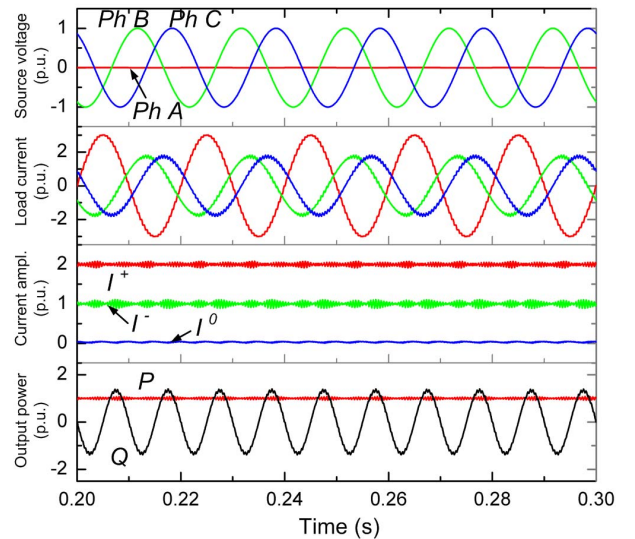
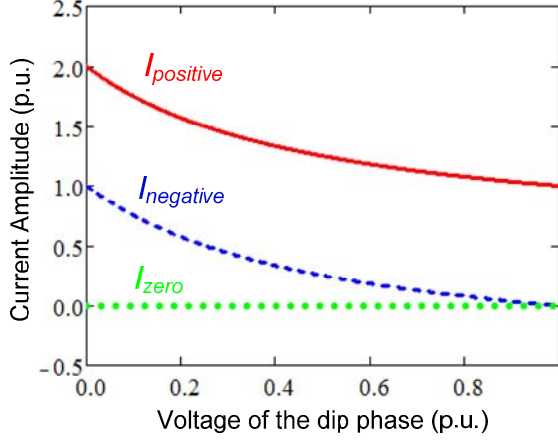
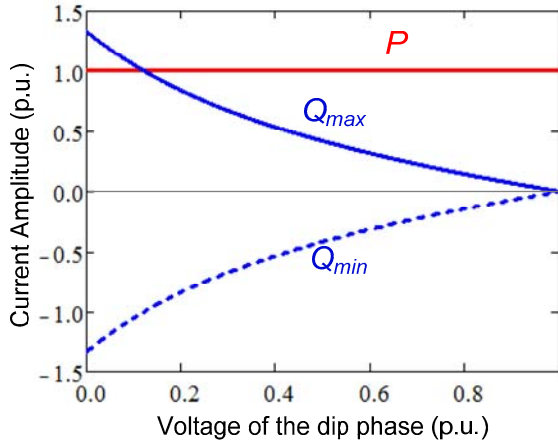


Fig. 6. Simulation of the converter control with no active power oscillation (three-phase three-wire converter, $P_{ref}=1$ p.u., $Q_{ref}=0$ p.u., $P_{s2}=0$ p.u., $P_{c2}=0$ p.u., $V_A=0$ p.u.)



(a) Sequence current amplitude vs. V_A .



(b) P and Q range vs. V_A .

Fig. 7. Profile of converter control with no active power oscillation (three-phase three-wire converter, $P_{ref}=1$ p.u., $Q_{ref}=0$ p.u., $P_{s2}=0$ p.u., $P_{c2}=0$ p.u.)

$$\begin{aligned} Q_{c2} = 0 & \quad P_{c2} = 0 & \quad P_{s2} = 0 \\ Q_{s2} = 0 & \quad Q_{s2} = 0 & \quad Q_{c2} = 0 \end{aligned} \quad (14) \quad (15) \quad (16)$$

III. CONVERTER SYSTEM WITH ZERO-SEQUENCE CURRENT PATH

As can be seen, in the typical three-phase three-wire converter structure, four control freedoms for load current seem not to be enough to achieve satisfactory performances

under unbalanced AC source (either significantly power oscillation or over-loaded and unbalanced current will be presented). Therefore, more current control freedoms may be needed in order to improve the control performance of the converter under adverse AC source conditions.

Another series of converter structure is shown in Fig. 8 (a) and Fig. 8 (b), with the control method in Fig. 9. Compared to the three-wire converter structure, these types of converters introduce zero sequence current path [24]-[26], which may enable extra current control freedoms to achieve better power control performance. It is noted that in the grid connected application, the zero sequence current is not injected into the grid but trapped in the typically used d - Y transformer.

With the zero sequence current, the three-phase current generated by the converter can be written as [27]-[19]:

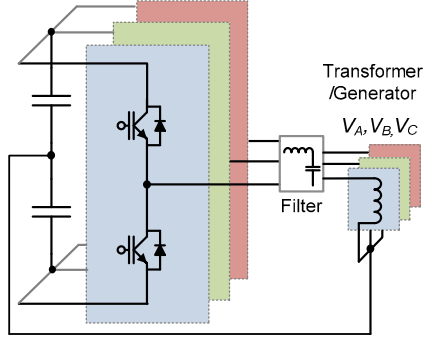
$$\mathbf{I}_C = \mathbf{I}^+ + \mathbf{I}^- + \mathbf{I}^0 \quad (17)$$

By operating the voltage of AC source (1) and current controlled by power converter (17), the instantaneous generated real power p , imaginary power q in the $\alpha\beta$ coordinate and the real power p_0 in the zero coordinate can be calculated as:

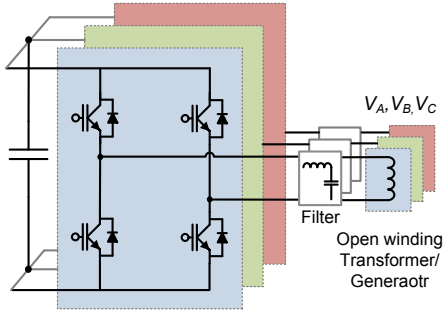
$$\begin{aligned} \begin{bmatrix} p \\ q \\ p_0 \end{bmatrix} &= \begin{bmatrix} v_\alpha \cdot i_\alpha + v_\beta \cdot i_\beta \\ v_\alpha \cdot i_\beta - v_\beta \cdot i_\alpha \\ v_0 \cdot i_0 \end{bmatrix} \\ &= \begin{bmatrix} \bar{P} + P_{c2} \cdot \cos(2\omega t) + P_{s2} \cdot \sin(2\omega t) \\ \bar{Q} + Q_{c2} \cdot \cos(2\omega t) + Q_{s2} \cdot \sin(2\omega t) \\ \bar{P}_0 + P_{0c2} \cdot \cos(2\omega t) + P_{0s2} \cdot \sin(2\omega t) \end{bmatrix} \end{aligned} \quad (18)$$

Then the instantaneous three-phase real power $p_{3\phi}$ and imaginary power $q_{3\phi}$ of the converter can be written as:

$$\begin{aligned} \begin{bmatrix} p_{3\phi} \\ q_{3\phi} \end{bmatrix} &= \begin{bmatrix} p + p_0 \\ q \end{bmatrix} \\ &= \begin{bmatrix} \bar{P} + \bar{P}_0 \\ \bar{Q} \end{bmatrix} + \begin{bmatrix} P_{c2} + P_{0c2} \\ Q_{c2} \end{bmatrix} \cos(2\omega t) \\ &\quad + \begin{bmatrix} P_{s2} + P_{0s2} \\ Q_{s2} \end{bmatrix} \sin(2\omega t) \end{aligned} \quad (19)$$



(a) Four-wire system



(b) Six-wire system

Fig. 8. Converter structure with zero sequence current path.

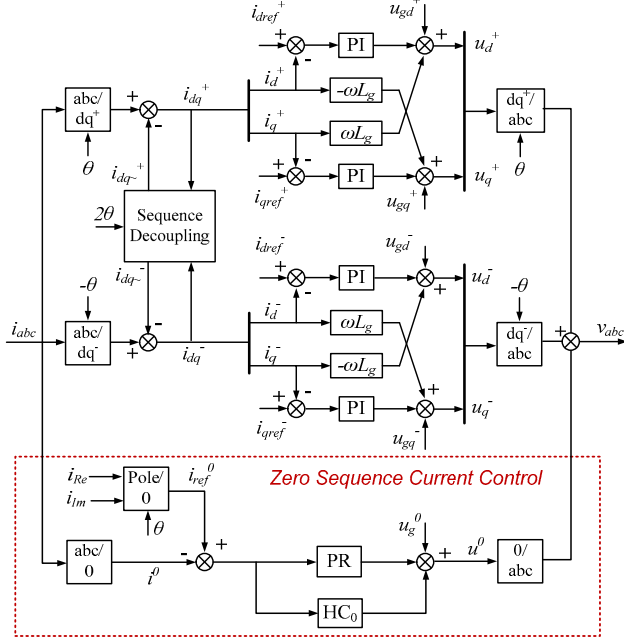


Fig. 9. Control structure for converter system with zero sequence current.

It is noted that the voltage and current in zero sequence only contribute to the real power $p_{3\phi}$ of the converter. Each part of (19) can be calculated as:

$$\begin{aligned} \bar{P} &= \frac{3}{2}(v_d^+ \cdot i_d^+ + v_d^- \cdot i_d^-) \\ P_{c2} &= \frac{3}{2}(v_d^- \cdot i_d^+ + v_d^+ \cdot i_d^-) \end{aligned} \quad (20)$$

$$\begin{aligned} P_{s2} &= \frac{3}{2}(-v_d^- \cdot i_q^+ + v_d^+ \cdot i_q^-) \\ \bar{Q} &= \frac{3}{2}(-v_d^+ \cdot i_q^+ - v_d^- \cdot i_q^-) \\ Q_{c2} &= \frac{3}{2}(-v_d^- \cdot i_q^+ - v_d^+ \cdot i_q^-) \end{aligned} \quad (21)$$

$$Q_{s2} = \frac{3}{2}(-v_d^- \cdot i_d^+ + v_d^+ \cdot i_d^-)$$

$$\bar{P}_0 = \frac{3}{2}(v_{Re}^0 \cdot i_{Re}^0) \quad (22)$$

$$P_{0c2} = \frac{3}{2}(v_{Re}^0 \cdot i_{Re}^0)$$

$$P_{0s2} = \frac{3}{2}(-v_{Re}^0 \cdot i_{Im}^0)$$

where the zero sequence voltage and current are more like a single phase AC component at fundamental frequency. They can be represented by the real part and imaginary part as:

$$\begin{aligned} v_{Re}^0 &= V^0 \cos(\varphi^0) = V^0 \\ v_{Im}^0 &= V^0 \sin(\varphi^0) = 0 \\ i_{Re}^0 &= I^0 \cos(\delta^0) \\ i_{Im}^0 &= I^0 \sin(\delta^0) \end{aligned} \quad (23)$$

It can be seen from (20)-(22) that if the three-phase AC source voltage is decided, then the converter has six controllable freedoms (i_d^+ , i_q^+ , i_d^- , i_q^- , i_{Re}^0 and i_{Im}^0) to regulate the current flowing in AC source. That means: six control targets/functions can be established by the converter using the zero sequence current path. Normally the three-phase average active and reactive power delivered by the converter are two basic requirements for a given application, then two control functions need to be first settled as:

$$\begin{aligned} \bar{P}_{3\phi} &= \bar{P} + \bar{P}_0 = P_{ref} \\ \bar{Q}_{3\phi} &= \bar{Q} = Q_{ref} \end{aligned} \quad (24)$$

So for the converter system with zero sequence current path, there are four control freedoms left to achieve two more control targets than the traditional three-wire system, which also means extended controllability and better performance under the unbalanced AC source.

A. Elimination of both active and reactive power oscillation.

Because of more current control freedoms, the power converter with zero sequence current path can not only eliminate the oscillation in the active power, but also cancel

the oscillation in the reactive power at the same time. This control targets can be written as:

$$\begin{aligned} P_{3\phi c2} = P_{c2} + P_{0c2} = 0 & & Q_{c2} = 0 \\ P_{3\phi s2} = P_{s2} + P_{0s2} = 0 & & Q_{s2} = 0 \end{aligned} \quad (25)$$

It can be seen that, the power oscillation caused by zero sequence current P_{0c2} and P_{0s2} are used to compensate the power oscillation P_{c2} and P_{s2} caused by the positive and negative sequence currents.

Translating the control targets in (24) and (25), all the controllable current components of the converter with zero sequence current path can be calculated as:

$$i_d^+ = \frac{2}{3} \cdot \frac{P_{ref}}{(v_d^+ - v_d^-) \cdot (1 - v_d^- / v_d^+)} \quad i_d^- = \frac{v_d^-}{v_d^+} \cdot i_d^+ \quad (26)$$

$$i_q^+ = \frac{2}{3} \cdot \frac{Q_{ref}}{-v_d^+ + (v_d^-)^2 / v_d^+} \quad i_q^- = -\frac{v_d^-}{v_d^+} \cdot i_q^+$$

$$i_{Re}^0 = \frac{2}{3} \cdot \frac{P_{ref} - \bar{P}}{v_{Re}^0} \quad (27)$$

$$i_{Im}^0 = \frac{v_d^+ \cdot i_q^- - v_d^- \cdot i_q^+}{v_{Re}^0}$$

When applying the current references in (26) and (27), the corresponding source voltage, load current, sequence current, and the instantaneous power delivered by converter are shown in Fig. 10. It can be seen that by this control strategy, the oscillation of both active and reactive power at twice of the fundamental frequency can be eliminated. Moreover, compared to the control strategies for three-wire system, the

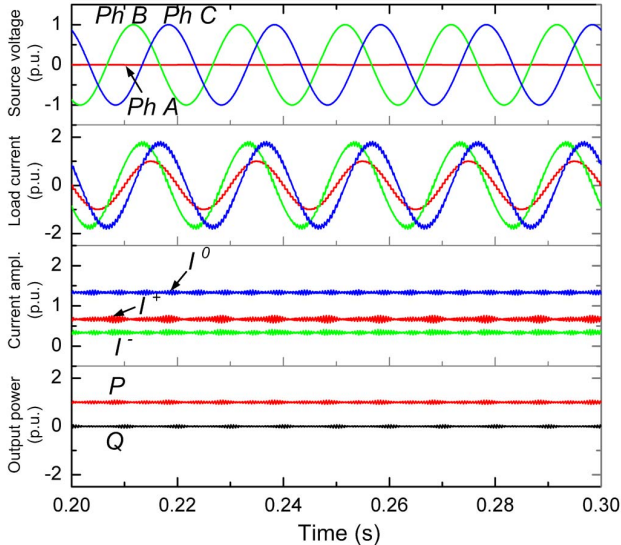
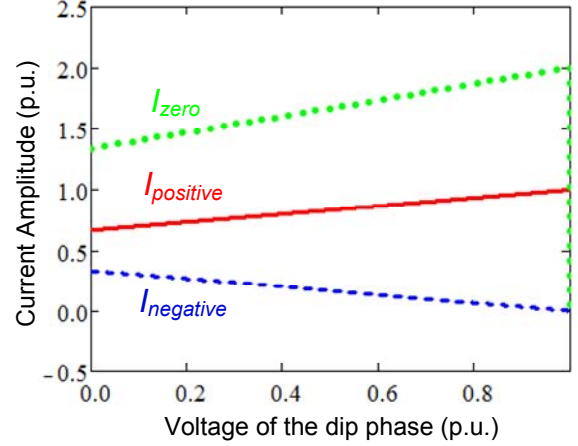
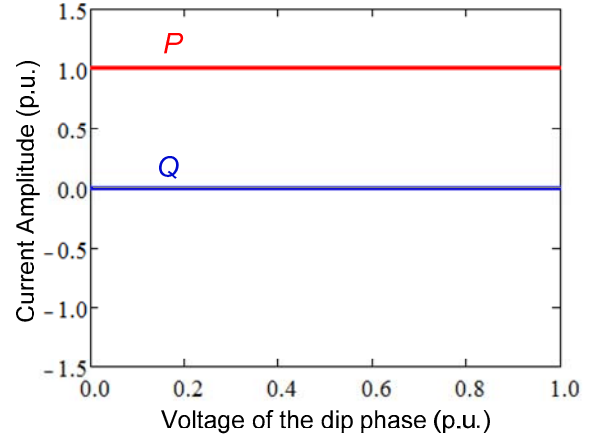


Fig. 10. Simulation of converter control with no active and reactive power oscillation (three phase converter with zero sequence path, $P_{ref}=1$ p.u., $Q_{ref}=0$ p.u., $P_{s2}=0$ p.u., $P_{c2}=0$ p.u., $Q_{s2}=0$ p.u., $Q_{c2}=0$ p.u., $V_A=0$ p.u.)



(a) Sequence current amplitude vs. V_A .



(b) P and Q ranges vs. V_A .

Fig. 11. Profile of converter control with no active and reactive power oscillation (three phase converter with zero sequence path, $P_{ref}=1$ p.u., $Q_{ref}=0$ p.u., $P_{s2}=0$ p.u., $P_{c2}=0$ p.u., $Q_{s2}=0$ p.u., $Q_{c2}=0$ p.u.)

amplitude of load current in each phase is not further increased, and the current in the faulty phase is smaller than the other two normal phases.

The current amplitude in different sequences, as well as the delivered active/reactive power with relation to the voltage amplitude of the dipping phase is shown in Fig. 11 (a) and Fig. 11 (b) respectively. It is noted that the converter has to deliver positive, negative and zero sequence currents to achieve this control strategy.

B. Elimination of active power oscillation and negative sequence current.

Another promising control strategy for the converter using zero sequence current path is to eliminate the active power oscillation and negative sequence current at the same time, the extra four control targets besides (24) can be written as:

$$\begin{aligned} P_{3\phi c2} = P_{c2} + P_{0c2} = 0 & & i_d^- = 0 \\ P_{3\phi s2} = P_{s2} + P_{0s2} = 0 & & i_q^- = 0 \end{aligned} \quad (28)$$

Translating the control targets in (24) and (28), all the controllable current components of the converter with zero sequence current path can be calculated as:

$$\begin{aligned} i_d^+ &= \frac{2}{3} \cdot \frac{P_{ref}}{(v_d^+ - v_d^-)} & i_d^- &= 0 \\ i_q^+ &= \frac{2}{3} \cdot \frac{Q_{ref}}{-v_d^+} & i_q^- &= 0 \end{aligned} \quad (29)$$

$$\begin{aligned} i_{Re}^0 &= \frac{-v_d^- \cdot i_d^+}{v_{Re}^0} \\ i_{Im}^0 &= 0 \end{aligned} \quad (30)$$

When applying the current references in (29) and (30), the corresponding source voltage, load current, sequence current, and the instantaneous power delivered by converter are shown in Fig. 12. It can be seen that by this control strategy, the oscillation of active power at twice of the fundamental frequency can be eliminated, and the load current in the faulty phase is reduced to zero.

The current amplitude in the different sequences, as well as the delivered active/reactive power with relation to the voltage on the dipping phase are shown in Fig. 13 (a) and Fig. 13 (b) respectively. It is noted that the converter has to deliver constant positive and zero sequence currents in order to achieve this control strategy under different dips of source voltage. The oscillation of reactive power is maintained in a much smaller range (up to ± 0.3 p. u.) compared to that in the

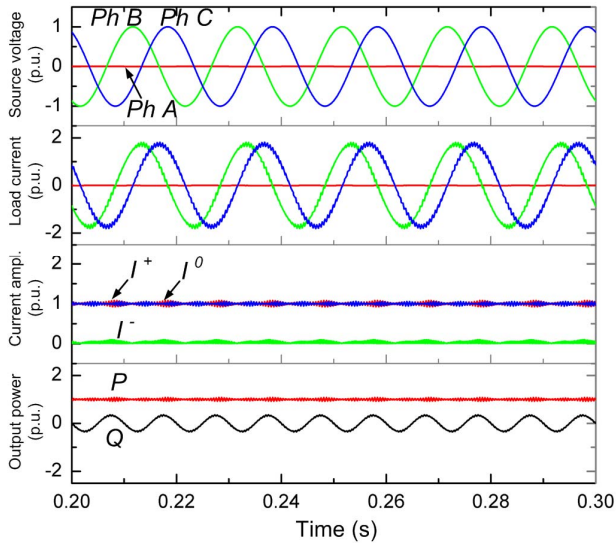
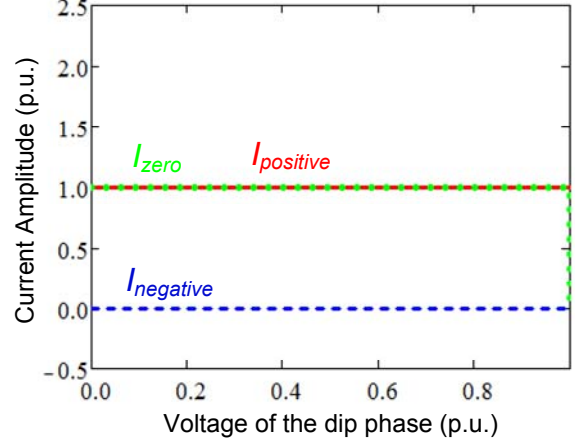
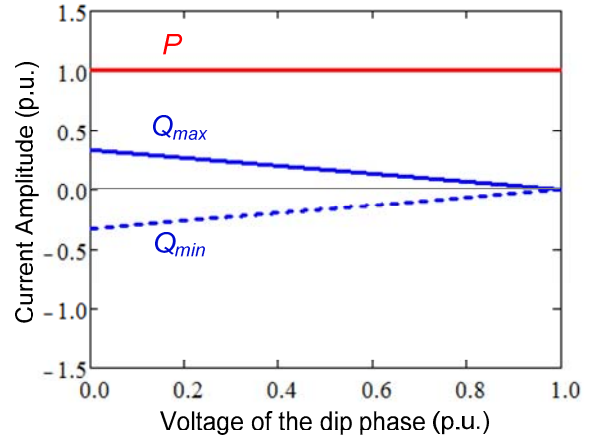


Fig. 12. Simulation of converter control with no active power oscillation and no negative sequence (three phase converter with zero sequence current path, $P_{ref}=1$ p.u., $Q_{ref}=0$ p.u., $P_{s2}=0$ p.u., $P_{c2}=0$ p.u., $i_d^-=0$ p.u., $i_q^-=0$ p.u., $V_A=0$ p.u.)



(a) Sequence current amplitude vs. V_A .



(b) P and Q ranges vs. V_A .

Fig. 13. Profile of converter control with no active power oscillation and no negative sequence (three phase converter with zero sequence current path, $P_{ref}=1$ p.u., $Q_{ref}=0$ p.u., $P_{s2}=0$ p.u., $P_{c2}=0$ p.u., $i_d^-=0$ p.u., $i_q^-=0$ p.u.)

three-wire system (up to ± 1.3 p. u.) in Fig. 7 (b).

The converter stresses for the active/reactive power oscillations and the current amplitude in the faulty/normal phases are compared in Table II, where different control strategies and converter structures are indicated respectively. It can be seen that by introducing the converter structures and controls with zero sequence current path, the power oscillations under unbalanced AC source are significantly reduced, meanwhile the current amplitude in the normal phases are not further stressed, and the current stress in the faulty phases are significantly relieved.

Table II. Converter stress comparison by different control strategies (values are represented in p.u., $P_{ref}=1$ p.u., $Q_{ref}=0$ p.u., $V_A=0$ p.u.).

Converter stress	Typical 3-wire		Zero-sequence	
	Control A	Control B	Control A	Control B
Active power osc. P_{osc}	0.5	0	0	0
Reactive power osc. Q_{osc}	0.5	1.3	0	0.3
Current in faulty phase I_{fault}	1.5	3	1	0
Current in normal phase I_{norm}	1.5	2	2	2

Typical 3-wire converter

Control A: no negative sequence current.

Control B: no active power oscillation.

Converter with zero sequence current path

Control A: no active and reactive power oscillations.

Control B: no active power oscillation and no negative seq.current.

IV. CONCLUSION

In a typical three-phase three-wire converter structure, there are four current control freedoms, and it may be not enough to achieve satisfactory performances under unbalanced AC source because either significantly oscillated power or over-loaded current will be presented.

In the three-phase converter structure with zero sequence current path, there are six current control freedoms. The extra two control freedoms coming from the zero sequence current can be utilized to extend the controllability of the converter and improve the control performance under unbalanced AC source. By the proposed control strategies, it is possible to totally cancel the oscillation in both the active and the reactive power, or reduced the oscillation amplitude in the reactive power. Meanwhile, the current amplitude of the faulty phase is significantly relieved without further increasing the current amplitude in the normal phases.

REFERENCE

[1] F. Blaabjerg, M. Liserre, K. Ma, "Power Electronics Converters for Wind Turbine Systems," *IEEE Trans. on Industry Applications*, vol. 48, no. 2, pp. 708-719, 2012.

[2] R. Teodorescu, M. Liserre, P. Rodriguez, Grid Converters for Photovoltaic and Wind Power Systems, Wiley-IEEE press, 2011.

[3] J. Rocabert, G.M.S. Azevedo, A. Luna, J.M. Guerrero, J.I. Candela, P. Rodríguez, "Intelligent Connection Agent for Three-Phase Grid-Connected Microgrids," *IEEE Trans. on Power Electronics*, Vol. 26, No. 10, pp. 2993-3005, 2011.

[4] J. W. Kolar, T. Friedli, "The Essence of Three-Phase PFC Rectifier Systems—Part 1," *IEEE Trans. on Power Electronics*, Vol. 28, No. 1, pp. 176-198, Jan 2013.

[5] Jiabing Hu, Lei Shang, Yikang He, Z.Z. Zhu, "Direct Active and Reactive Power Regulation of Grid-Connected DC/AC Converters Using Sliding Mode Control Approach," *IEEE Trans. on Power Electronics*, Vol. 26, No. 1, pp. 210-222, Jan 2011.

[6] C. Wessels, F. Gebhardt, F.W. Fuchs, "Fault Ride-Through of a DFIG Wind Turbine Using a Dynamic Voltage Restorer During Symmetrical and Asymmetrical Grid Faults," *IEEE Trans. on Power Electronics*, Vol. 26, No. 3, pp. 807-815, Mar 2011.

[7] F. Aghili, "Fault-Tolerant Torque Control of BLDC Motors," *IEEE Trans. on Power Electronics*, Vol. 26, No. 2, pp. 355-363, Feb 2011.

[8] Yan Xiangwu, G. Venkataramanan, Wang Yang, Dong Qing, Zhang Bo, "Grid-Fault Tolerant Operation of a DFIG Wind Turbine Generator Using a Passive Resistance Network," *IEEE Trans. on Power Electronics*, Vol. 26, No. 10, pp. 2896-2905, Oct 2011.

[9] B.A. Welchko, T.A. Lipo, T.M. Jahns, S.E. Schulz, "Fault tolerant three-phase AC motor drive topologies: a comparison of features, cost, and limitations," *IEEE Trans. on Power Electronics*, Vol. 19, No. 4, pp. 1108- 1116, 2004.

[10] F. Blaabjerg, K. Ma, D. Zhou, "Power electronics and reliability in renewable energy systems", *Proc. of ISIE 2012*, pp. 19 - 30, May 2012.

[11] Yantao Song, Bingsen Wang, "Survey on Reliability of Power Electronic Systems," *IEEE Trans. on Power Electronics*, Vol. 28, No. 1, pp. 591-604, 2013.

[12] M. Altin, O. Goksu, R. Teodorescu, P. Rodriguez, B. Bak-Jensen, L. Helle, "Overview of recent grid codes for wind power integration," *Proc. of OPTIM'2010*, pp.1152-1160, 2010.

[13] E.ON-Netz – Grid Code. High and extra high voltage, April 2006.

[14] P. Rodríguez, A. Luna, R. Muñoz-Aguilar, I. Etxeberria-Otadui, R. Teodorescu, F. Blaabjerg, "A Stationary Reference Frame Grid Synchronization System for Three-Phase Grid-Connected Power Converters Under Adverse Grid Conditions," *IEEE Trans. on Power Electronics*, Vol. 27, No. 1, pp. 99-112, Jan 2012.

[15] A.J. Roscoe, S.J. Finney, G.M. Burt, "Tradeoffs Between AC Power Quality and DC Bus Ripple for 3-Phase 3-Wire Inverter-Connected Devices Within Microgrids," *IEEE Trans. on Power Electronics*, Vol. 26, No. 3, pp. 674-688, Mar 2011.

[16] C.H. Ng, Li Ran, J. Bumby, "Unbalanced-Grid-Fault Ride-Through Control for a Wind Turbine Inverter," *IEEE Trans. on Industry Applications*, vol. 44, no. 3, pp. 845-856, 2008.

[17] P. Rodríguez, A.V. Timbus, R. Teodorescu, M. Liserre, F. Blaabjerg, "Flexible Active Power Control of Distributed Power Generation Systems During Grid Faults," *IEEE Trans. on Industrial Electronics*, vol. 54, no. 5, pp. 2583-2592, 2007.

[18] H. Song, K. Nam, "Dual current control scheme for PWM converter under unbalanced input voltage conditions," *IEEE Trans. on Industrial Electronics*, vol. 46, no. 5, pp. 953-959, 1999.

[19] H. Akagi, Y. Kanazawa, A. Nabae, "Instantaneous Reactive Power Compensators Comprising Switching Devices without Energy Storage Components," *IEEE Trans. on Industry Applications*, vol. IA-20, no. 3, pp. 625-630, 1984.

[20] J. Miret, M. Castilla, A. Camacho, L. Vicuña, J. Matas, "Control Scheme for Photovoltaic Three-Phase Inverters to Minimize Peak Currents During Unbalanced Grid-Voltage Sags," *IEEE Trans. on Power Electronics*, Vol. 27, No. 10, pp. 4262-4271, Oct 2012.

[21] F. González-Espín, G. Garcerá, I. Patrao, E. Figueres, "An Adaptive Control System for Three-Phase Photovoltaic Inverters Working in a Polluted and Variable Frequency Electric Grid," *IEEE Trans. on Power Electronics*, Vol. 27, No. 10, pp. 4248-4261, Oct 2012.

[22] G. Saccomando, J. Svensson, A. Sannino, "Improving voltage disturbance rejection for variable-speed wind turbines," *IEEE Trans. on Energy Conversion*, vol. 17, no. 3, pp. 422-428, 2002.

[23] N. Kaminski, A. Kopta, "Failure rates of HiPak Modules due to cosmic rays," ABB application note 5SYA 2042-04, Mar 2011.

[24] S. Sharma, B. Singh, "Performance of Voltage and Frequency Controller in Isolated Wind Power Generation for a Three-Phase Four-Wire System," *IEEE Trans. on Power Electronics*, Vol. 26, No. 12, pp. 3443-3452, Dec 2011.

[25] K. Ma, F. Blaabjerg, M. Liserre, "Thermal Analysis of Multilevel Grid Side Converters for 10 MW Wind Turbines under Low Voltage Ride Through," *IEEE Industry Applications Magazine*, 2013. (*Proc. of ECCE' 2011*, pp. 2117-2124, 2011.)

[26] J. Holtz, N. Oikonomou, "Optimal Control of a Dual Three-Level Inverter System for Medium-Voltage Drives," *IEEE Trans. on Industry Applications*, vol. 46, no. 3, pp. 1034-1041, 2010.

[27] E.H. Watanabe, R.M. Stephan, M. Aredes, "New concepts of instantaneous active and reactive powers in electrical systems with generic loads," *IEEE Trans. on Power Delivery*, vol. 8, no. 2, pp. 697-703, 1993.

[28] M. Aredes, E.H. Watanabe, "New control algorithms for series and shunt three-phase four-wire active power filters," *IEEE Trans. on Power Delivery*, vol. 10, no. 3, pp. 1649-1656, 1995.

[29] M. Aredes, J. Hafner, K. Heumann, "Three-phase four-wire shunt active filter control strategies," *IEEE Trans. on Power Electronics*, vol. 12, no. 2, pp. 311-318, 1997.